Facial morphology in the adult Spanish population: a comprehensive anthropometric study using 3D photoanthropometry

Rubén Martos[1†], Belén Navarro-López[2,3,4†], Victoria Suarez-Ulloa[5], Enrique Bermejo[5,6], Begoña Martínez-Jarreta[7], Susana Jiménez[8], Marian M. de Pancorbo[2,7]

[1] Department of Legal Medicine, Toxicology and Physical Anthropology, University of Granada, Granada (Spain)

[2] BIOMICs Research Group, Lascaray Research Center, University of the Basque Country UPV/EHU, Vitoria-Gasteiz (Spain)

[3] Department of Zoology and Animal Cellular Biology, Faculty of Pharmacy, University of the Basque Country UPV/EHU, Vitoria-Gasteiz (Spain)

[4] Bioaraba Health Research Institute, Vitoria-Gasteiz (Spain)

[5] Panacea Cooperative Research S. Coop, Castilla y León (Spain)

[6] Department of Computer Science and Artificial Intelligence, University of Granada, Granada (Spain)

[7] Faculty of Medicine, University of Zaragoza, Zaragoza (Spain)

[8] Department of Pathology and Surgery, University of Miguel Hernández, Alicante (Spain)

[†] Rubén Martos and Belén Navarro - López contributed equally to this work

SUMMARY

This study elucidates the anthropometric variations of the Spanish facial features through the presentation of extensive adult population reference data derived from photoanthropometric measurements and indices. A total of 535 Spanish individuals (215 men and 320 women) of legal age participated in this research. Using 3D facial images captured by a portable white light led 3D scanner, 21 cephalometric landmarks were identified. Subsequently, 21 linear measurements and 20 proportionality indices of the head and face based on standard traditional measurements, were calculated. Descriptive statistics, including the mean value, standard deviation, minimum value, maximum value, and the first, second, and third quartiles were determined for each measurement and index. Furthermore, potential differences between sexes (male and female) and age group (young adulthood and the middle/older adulthood), as well as associations between measurements and body mass index were assessed. Results revealed statistically significant differences between male and female individuals in 25 of the 27 measurements, with male exhibiting higher means. Significant differences were observed in 11 of the 21 indices studied, with six higher in males and five higher in females. Correlation analysis between measures and indices with BMI showed a weak statistically significant association with lower facial area. Age group comparisons indicated significant differences in over half of the variables analyzed, predominantly affecting the eyes, nose, mouth, and mandible. These findings

Corresponding author:
Dr. Rubén Martos. Departamento de Medicina Legal, Toxicología y Antropología Física. Universidad de Granada. Área de Antropología Física: Torre A, 4º planta, Avda. de la Investigación 11, 18016 Granada, Spain. Phone: 644408855. E-mail: rmarfer89@gmail.com

Submitted: October 28, 2024. **Accepted:** March 15, 2025

https://doi.org/10.52083/TSZP2709

contribute to the establishment of reference anthropometric data for the Spanish population and underscore the importance of tailored approaches in facial morphological studies to ensure the generation of accurate and applicable results.

Key words: Craniofacial anthropometry – Facial analysis – 3D Photoanthropometry – Facial features – Spanish population

INTRODUCTION

The human face exhibits remarkable morphological diversity, which not only defines individual identity but also provides valuable insights into various aspects such as disposition, general health, and stress levels (Mane et al., 2010). While facial phenotypes are inherently linked to the biological traits of specific populations, they are also influenced by environmental factors. This has driven research to focus on identifying facial traits that can serve as distinguishing individual markers. Facial analysis, which stems from disciplines such as medicine, aesthetics, and anthropology, plays a vital role in forensic science, orthodontics, clinical genetics, maxillofacial surgery, and plastic surgery (Dong et al., 2011; Matthews et al., 2021; Menéndez López-Mateos et al., 2019; Ogawa et al., 2015). Additionally, the growing demand for facial plastic surgeries has spurred the development of precise measurements of the soft tissue profile, including linear and angular assessments, as well as cephalometric analyses to determine ideal facial proportions (Farkas, 1994).

Craniofacial anthropometry, which measures linear distances, proportions, angles, and ratios, has emerged as an efficient and cost-effective method for quantitatively analyzing craniofacial morphology (Bergman, 1999; Farkas, 1996). This technique is particularly useful for population studies due to the existence of comparative databases (Farkas et al., 2005). However, significant variation in facial proportions across different populations underscore the need for specific normative data.

In recent years, digital methods of facial anthropometry, particularly 3D photoanthropometric analysis, have gained prominence as a non-invasive technique. By using cephalometric landmarks on facial images, this method measures linear measurements and proportional indices to quantify facial features and proportions (Mai et al., 2020). It proves to be a valuable tool in capturing anthropometric data that helps understand the specific morphological variations within a population. Thus, having basic statistical data for anthropometric measurements is crucial (Baik et al., 2007; Dong et al., 2011; Farkas et al., 2005; Jahanshahi et al., 2008; Mane et al., 2010; Ozdemir et al., 2009; Virdi et al., 2019). Standardized reference data allow for the identification and evaluation of facial traits that deviate from the norm within a given population.

Several studies around the world have sought to establish reference data for populations using 3D photoanthropometry (Baik et al., 2007; Dong et al., 2011; Menéndez López-Mateos et al., 2019; Ogawa et al., 2015), relying on non-invasive systems to capture 3D facial images. Unlike traditional anthropometry, which requires subjects to remain still for several minutes and involves physical contact, 3D photoanthropometry captures and stores the facial shape in a matter of seconds without contact. This rapid acquisition reduces the likelihood of measurement errors caused by movement or surface alterations and minimizes stress for both subjects and observers by streamlining the process.

In addition to the use of traditional cephalometric landmarks for measuring linear distances between specific points and calculating indices in the facial 3D model to quantify facial features and proportions, recent advances in methodology have introduced more sophisticated techniques for assessing facial shape. One such approach involves the use of a quasi-landmark mesh (Claes et al., 2014; Matthews et al., 2023).

Despite Spain's diverse population, there has been only one study addressing facial anthropometric variations in the Southern Spanish region, involving a cohort of 100 volunteers and a 3D photographic device for orthodontic purposes (Menéndez López-Mateos et al., 2019).

This study aims to expand upon this by providing a comprehensive reference of facial morphological characteristics in the Spanish population.

A sample of 535 adult volunteers from different regions of the country was used to acquire 3D facial images, resulting in the generation of basic statistical data for 48 anthropometric linear measurements and indices, along with detailed distributions of these measurements.

MATERIAL AND METHODS

For the conduct of this study, a sample of 535 healthy adult volunteers of both sexes (215 men and 320 women) and of legal age were enrolled (Table 1). All the participants were of European ancestry and belonged to the Spanish population. The majority of the individuals originated from the Basque and Valencian regions, though individuals from other regions, including Andalucia, Murcia, Cataluña, the Balearic Islands, Aragon, Navarra, La Rioja, Cantabria, Asturias, Galicia, Extremadura, Castilla-La Mancha, Castilla y León, and Madrid, were also represented. Information regarding geographic origin, age, sex, body mass index and facial traumas or surgeries was obtained using a questionnaire. However, given the impact of internal migration within Spain, resulting in interregional admixture due to individuals relocating for employment or other socioeconomic reasons, birthplace information alone was deemed insufficient for accurately determining geographic region. To mitigate potential misclassification of geographic origin and considering that many individuals have maternal and paternal lineages from different Spanish regions, the study population was treated as a genetically homogeneous unit. Consequently, geographic region was excluded as a variable in the analysis, with only sex, age, and BMI being considered.

Those volunteers who had a medical history of facial surgery, craniofacial anomalies, pathologies, trauma, or cosmetic facial aesthetic procedure that could have altered the facial morphology were removed from the sample.

Participants voluntarily offered to take part in the study after receiving a detailed explanation of the protocol and expressed their consent to participate by signing an ethics committee-approved informed consent form. Ethical approval for this study (M10_2021_143) was provided by the Ethics Committee for Research on Human Subjects of the University of the Basque Country, CEISH-UPV/EHU, BOPV 32, 17/2/2014.

Three-dimensional image acquisition procedure

The three-dimensional facial images of each volunteer were obtained using a portable white light led 3D scanner Academia 3D/20 (Creaform, Canada) by a single operator, following the published protocols by the 3D Facial Norms (3DFN) project (Weinberg et al., 2016) and Heike et al. (2010).

Prior to facial imaging, participants were asked, when necessary, to remove any accessories that might disturb the scanning and to tie back their hair to avoid covering their ears and forehead. 3D images were taken with the subjects in a seated position, with the head forward and slightly tilted back to ensure adequate coverage of the region under the nose and chin. To measure the distances that characterize the morphology of the face, participants were also instructed to keep their face relaxed with a neutral expression, closing gently their eyes and lips. Each scan was inspected in situ to ensure 3D surface quality. Additional captures were obtained until one of sufficient quality was acquired, as needed.

Images obtained from the 3D scans were inspected with the ACADEMIA Software Bundle (VXmodel, VXinspect and VXElements) to check their initial quality and remove background noise. Cleaning consisted of discarding extraneous data from the models, including hair and parts of the neck and shoulders. Each cleaned 3D image was

Table 1. Age distribution of samples.

Age range	Male (N = 215)		Female (N= 320)	
	N	(%)	N	(%)
Young adulthood (18 – 35)	164	76.28	237	74.06
Middle age (36 – 60)	41	19.07	83	25.94
Older adulthood (> 60)	10	4.65	0	0.00

exported as an Object Wavefront (.obj) file.

Cephalometric landmark's location procedure

To perform a metric assessment of the Spanish population facial morphology we have selected a set of 21 cephalometric landmarks (11 unilateral and 10 bilateral, 31 in total) (Table 2) to estimate 21 linear measurements (Table 3) and 20 proportionality indices (Table 4) of the head and face based on standard anthropometric measurements traditionally used in anthropology (Farkas, 1994; Martin, 1957).

The localization of the 31 cephalometric landmarks in the 535 facial 3D models has been achieved through the adaptation of the automatic method proposed by (Bermejo et al., 2021). This method employs a hybrid structure, utilizing a deformable template to initialize landmark positions. Following this automatic initialization, a manual refinement stage is conducted by an expert to ensure precise localization based on standardized definitions.

The automatic method, rooted in the Meshmonk registration framework (White et al., 2019), is employed to generate an initial set of landmarks for each facial 3D model. The procedure follows a template-based strategy, involving the alignment and elastic deformation of a reference 3D mesh to create a homologous model of the target mesh (non-rigid registration). This homologous surface establishes correspondence between the vertices of the template and the target surface, allowing landmarks on the template to be projected onto anatomically equivalent points of the target sur-

Table 2. List of cephalometric landmarks employed in this study.

Nº	Landmark	Abv	Definition
1	Alare	al'	The most lateral point on the nasal ala.
2	Cheilion	ch'	Outer corners of the mouth where the outer edges of the upper and lower vermilions meet.
3	Endocanthion	en'	Most medial point of the palpebral fissure, at the inner commissure of the eye; best seen when subject is gazing upward.
4	Exocanthion	ex'	Most lateral point of the palpebral fissure, at the outer commissure of the eye; best seen when subject is gazing upward.
5	Frontotemporale	ft'	Point of concavity on each side of the forehead above the supraorbital rim, lateral to the elevation of the linea temporalis.
6	Frontozygomaticus	fz'	Most lateral point on the frontozygomatic suture, identified by palpation of the suture line at the superolateral corner of the orbit.
7	Glabella	g'	Most anterior midline point on the forehead, in the region of the superciliary ridges.
8	Gnathion	gn'	Median point halfway between pg′ and me'.
9	Gonion	go'	Most lateral point on the mandibular angle, adjacent to go, identified by palpation.
10	Labiale inferius	li'	Midpoint of the vermilion border of the lower lip (identical to labrale inferius).
11	Labiale superius	ls'	Midpoint of the vermilion border of the upper lip (not identical to and not to be confused for labrale superius).
12	Menton	me'	Most inferior median point of the chin.
13	Midsupraorbital	mso'	Point anteriorly adjacent to the superior orbital rim, at a line that vertically bisects the orbit.
14	Nasion	n'	Point directly anterior to the nasofrontal suture, in the midline, overlying n.
15	Otobasion inferius	obi'	Most inferior point of attachment of the ear lobe with the cheek.
16	Pogonion	pg'	Most anterior midpoint of the chin, located on the skin surface anterior to the identical bony landmark of the mandible.
17	Pronasale	prn'	The most anteriorly protruded point of the apex nasi. In the case of a bifid nose, the more protruding tip is chosen.
18	Stomion	sto'	Midline point of the labial fissure when the lips are closed naturally, with teeth shut in the natural position; if not in the midline, then below the philtrum.
19	Subnasale	sn'	Median point at the junction between the lower border of the nasal septum and the philtrum area.
20	Supramentale	sm'	Deepest midline point of the mentolabial sulcus.
21	Zygion	zy'	Most lateral point overlying each zygomatic arch, identified as the point of maximum bizygomatic breadth of the face.

Table 3. Linear measurements employed in this study.

Number	Absolute measurements	Abv
1	Orbital face height	en' L/R - gn'
2	Face height	n' - gn'
3	Upper face height	n' - sto'
4	Lower face depth	obi' L/R - gn'
5	Mid-face depth	obi' L/R - sn'
6	Lower chin height	pg' - gn'
7	Chin height	sm' - gn'
8	Lower face height	sn' - gn'
9	Mandible height	sto' - gn'
10	Intercanthal width	en' – en'
11	Eye fissure width	ex' L/R – en' L/R
12	Biocular width	ex' – ex'
13	Nose width	al' – al'
14	Nasal bridge length	n' - prn'
15	Nose height	n' - sn'
16	Nasal tip protrusion	sn' - prn'
17	Mouth width	ch' – ch'
18	Half mouth width	ch' L/R - sto'
19	Upper vermillion height	ls' - sto'
20	Lower vermillion height	li' - sto'
21	Distance mso-gn	mso' L/R - gn'

Table 4. Anthropometric indices employed in this study.

Number	Anthropometric indices	Abv
1	Intercanthal index	en' - en' / ex' - ex' x 100
2	Nose-face height index	n' - sn' / n' - gn' x 100
3	Nasal index	al' - al' / n' - sn' x 100
4	Intercanthal-nasal width index	en' - en' / al' - al' x 100
5	Nose-mouth width index	al' - al' / ch' - ch' x 100
6	Upper face-face height index	n' - sto' / n' - gn' x 100
7	Mandibulo-face height index	sto' - gn' / n' - gn' x 100
8	Mandibulo-upper face height index	sto' - gn' / n' - sto' x 100
9	Mandibulo-lower face height Index	sto' - gn' / sn' - gn' x 100
10	Orbital width index	ex' - en' / en' - en' x 100
11	Nasal tip protrusion-width index	sn' - prn' / al' - al' x 100
12	Nasal tip protrusion-height index	sn' - prn' / n' - sn' x 100
13	Upper lip height-mouth index	sn' - sto' / ch' - ch' x 100
14	Vermilion height index	ls' - sto' / sto' - li' x 100
15	Nasal bridge index	n' - prn' / n' - sn' x 100
16	Upper face height-biocular width index	n' - sto' / ex' - ex' x 100
17	Intercanthal width-upper face height index	en' - en' / n' - sto' x 100
18	Intercanthal-mouth width index	en' - en' / ch' - ch' x 100
19	Upper lip-face height index	sn' - sto' / sn' - gn' x 100
20	Lower lip-face height index	sto' - sm' / sn' - gn' x 100
21	Distance mso-gn	mso' L/R - gn'

face. The vertex index of the template landmark is known, enabling the determination of the corresponding 3D coordinate after elastic deformation. Consequently, the new 3D spatial location for each landmark is directly mapped onto the nearest vertex of the target surface.

The next step involves an expert carrying out manual refinement. The initialization coordinates of the landmarks for each 3D model, provided by the automatic method, were imported into the Skeleton-IDTM software. This software facilitates visualization of facial 3D models and allows the adjustment of landmark positions using a set of tools designed to enhance procedural accuracy (Martos et al., 2024). All images were refined by a single experienced observer following the standard landmarks definitions proposed by Caple and Stephan (2016) (Fig. 1).

To test for intra-observer reliability, 20 randomly selected 3D facial models were annotated manually in three rounds by the observer in intervals of two weeks. To test for inter-observer reliability, the same 20 images were annotated by another independent expert. Finally, to verify the accuracy of the refined automatic template fitting method, the dispersion against the expert manual marking has been studied in the same images.

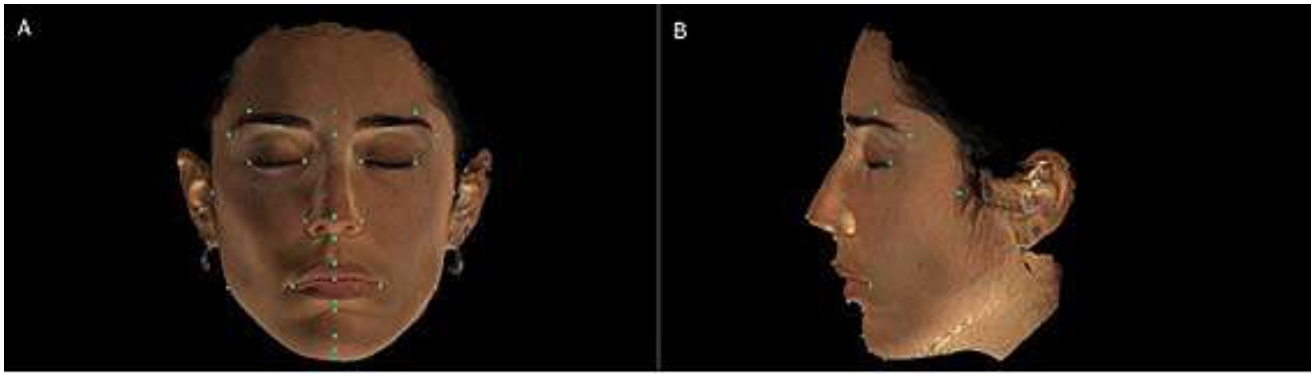

Fig. 1.- Frontal view (A) and profile view (B) of a female volunteer 3D model with all landmarks positioned.

Photo-anthropometric procedure

Once the expert had refined manually the landmarks in all 3D images, their Cartesian coordinates (x-axis, y-axis, z-axis) were exported as CSV files. Anthropometric linear measurements (Table 3) were computed by determining the distances between two landmarks in the 3D Cartesian coordinate system. To calculate the projected distance between two landmarks, given their x,y,z Cartesian coordinates as (x1, y1, z1) and (x2, y2, z2), the following formula was used:

$$Distance = \sqrt{(x1 - x2)^2 + (y1 - y2)^2 + (z1 - z2)^2}$$

Then, the anthropometric indices (Table 4) were derived from the linear measurements results according to their definitions.

For each measurement, descriptive statistics including the mean value, standard deviation (SD), minimum and maximum value, and the first, second, and third quartiles were determined. Statistical analyses were performed using IBM SPSS Statistics v25. Furthermore, one-sample Kolmogorov-Smirnov tests were carried out to verify whether the data adhered to a normal distribution.

Potential differences between sexes (male and female) were assessed. For measurements following a normal distribution, Student's t-test was used, while for non-normal data the Mann-Whitney U-test was employed. Association between measurements and body mass index (BMI) was also studied using Pearson and Spearman correlation coefficients, depending on whether the variables followed a normal distribution or not, respectively. Correlation coefficient values between 0-0.10 were considered as no correlation, between 0.10-0.40 weak correlation, between 0.40-0.60 moderate correlation, between 0.60-0.80 moderate-high correlation and between 0.80-1 high correlation. Finally, the effect of aging

on facial morphology was examined by comparing different age groups based on the age ranges presented in Table 1. Given the non-homogeneous sample distribution, the middle-aged and older adulthood categories were merged, allowing for comparisons between young adulthood and the combined middle/older adulthood group. Statistical comparisons were conducted separately for the overall sample and for males and females to determine potential sex-specific differences. As with the sex-based analysis, Student's t-test was applied to normally distributed variables, whereas the Mann-Whitney U-test was used for non-normally distributed data. The significance level in all analyses was set considering P-values < 0.01.

RESULTS

The variability scores for the dispersion analysis of cephalometric landmark localization are presented in millimeters, with values detailed across the 31 landmarks (Table 5 and supplementary Fig. S1). The inter-observer dispersion demonstrated a mean error of 3.307 mm, with 17 landmarks exhibiting localization errors exceeding 2 mm. In contrast, the intra-observer error for expert manual annotation showed a lower mean error of 1.459 mm, with the highest dispersion observed at the zygion and gonion landmarks (mean error > 2 mm). The refined automatic localization method yielded a mean error of 2.174 mm.

The relatively high inter-observer standard deviation suggests considerable variability among observers. The greatest dispersion has occurred in the localization of the zygion, gonion, and exocanthion landmarks (mean error > 4 mm). Regarding intra-observer dispersion, the mean and median show a smaller discrepancy compared to the inter-observer, suggesting greater precision and consistency by the same observer. Finally, the refined automatic method shows intermediate precision between observer variability and single observer consistency.

Based on refined automatic method results, landmarks with the highest localization errors, including frontotemporale, frontozygomaticus, gonion, menton, and zygion, were excluded from subsequent analyses.

Tables 6-9 show the mean, standard deviation, minimum and maximum value, and the first, second (median) and third quartiles for all the anthropometrical linear measurements and indices included in the study for males and females. Additionally, to obtain a more comprehensive insight into the distributions of these anthropometric linear measurements and indices, a Kolmogorov-Smirnov test was employed to assess their normality. For males, normality was rejected for the lower chin height, the right eye fissure width, and the vermilion height index. In the case of females, normality was rejected for the upper vermilion height, the nasal index, the orbital width index L/R, and the lower lip-face height index.

Tables 10-13 show the comparison of all the anthropometrical variables included in the study between male and female subjects, the correlation analysis between measures and indices with BMI, and the comparisons between young adulthood and middle/older adulthood. Statistically significant differences were found between male and female subjects in 36 of the 48 measurements. On the one hand, of the total of 27 absolute measurements, 25 of them exhibited significant differences, with male individuals showing a higher mean in all of them (supplementary Fig. S2). On the other hand, significant differences were observed in only 11 of the 21 indices studied. Of these, six indices were higher in males than in females (intercanthal index, nasal index, nose-mouth width index, mandibulo-face height index, mandibulo-upper face height index, and upper lip height index). The remaining five indices were higher in female subjects (nose-face height index, intercanthal-nasal width index, upper face-face height index, orbital width index L, and nasal tip protrusion-width index) (supplementary Fig. S3).

Correlation analysis between measures and indices with BMI showed statistically significant associations with nine variables (supplementary Fig. S4). However, all of these correlations were weak.

Comparative analysis across age groups revealed statistically significant differences in 14 out of 27 linear measurements and 12 out of 21

indices examined (supplementary Figs. S5 and S6, respectively). Notably, nine significant differences in linear measurements and seven in indices were consistently observed in both males and females when analyzed separately to assess potential sex-specific variations. When evaluating age-related differences between males and females, statistically significant differences were identified in mouth width exclusively among females (supplementary Fig. S7).

DISCUSSION

The findings of this study underscore the importance of considering population variability when diagnosing and planning treatment for orthognathic or craniofacial reconstructive surgery procedures. Applying normative anthropomet-

Table 5. Variability scores for the dispersion analysis of cephalometric landmark localization (in mm).

	Inter-observer		Intra-observer		Refined method	
Landmark Name	**Mean**	**SD**	**Mean**	**SD**	**Mean**	**SD**
Alare' L	1.284	0.513	2.671	1.086	1.367	0.549
Alare' R	1.045	0.368	3.880	1.792	1.743	1.350
Cheilion' L	0.907	0.568	1.125	0.697	1.085	0.787
Cheilion' R	0.835	0.409	0.684	0.549	0.752	0.744
Endocanthion' L	0.744	0.497	1.456	0.866	0.785	0.666
Endocanthion' R	0.606	0.276	1.429	0.821	0.763	0.330
Exocanthion' L	1.332	0.661	5.614	2.361	1.474	0.955
Exocanthion' R	1.021	0.558	5.059	2.273	1.048	1.020
Frontotemporale' L	1.930	0.636	2.897	1.564	4.028	2.204
Frontotemporale' R	1.884	0.909	5.338	3.726	3.544	2.035
Frontozygomaticus' L	1.807	0.634	3.262	2.333	3.386	1.249
Frontozygomaticus' R	1.608	0.598	3.632	2.833	2.854	1.336
Glabella	1.434	0.597	2.083	1.180	1.865	0.889
Gnathion'	1.439	0.716	1.723	0.924	2.100	1.355
Gonion' L	4.227	1.537	11.747	5.032	6.421	4.580
Gonion' R	4.289	1.737	10.998	4.552	6.401	3.386
Labiale Inferius'	0.800	0.541	0.942	0.599	1.059	0.760
Labiale Superius'	0.641	0.296	1.263	0.688	1.559	0.519
Menton	1.595	0.896	3.105	2.092	2.952	1.656
Midsupraorbital' L	1.054	0.289	2.058	1.151	1.577	0.787
Midsupraorbital' R	0.993	0.441	2.108	1.242	1.693	0.750
Nasion'	1.056	0.482	1.322	0.815	1.265	0.542
Otobasion Inferius' L	1.290	0.979	2.550	1.287	1.630	1.908
Otobasion Inferius' R	1.053	0.505	2.416	2.215	1.186	0.937
Pogonion	1.590	0.748	2.703	1.526	2.144	1.352
Pronasale'	0.843	0.414	0.929	0.576	1.279	0.606
Stomion'	0.645	0.196	0.966	0.529	0.799	0.404
Subnasale'	0.645	0.268	1.090	0.642	0.716	0.337
Supramentale'	0.706	0.366	1.354	0.740	1.066	0.686
Zygion' L	2.945	1.397	8.249	3.604	4.280	2.804
Zygion' R	2.967	1.432	7.853	4.113	4.472	2.782
Mean	**1.458**	**0.660**	**3.306**	**1.755**	**2.170**	**1.298**

Table 6. Basic statistics of Spanish male anthropometric linear measurements and P-values for Kolmogorov-Smirnov test.

Anthropometric linear measurements	Abv	Descriptive								Kolmogorov-Smirnov
		N	Mean	SD	Minimun	Maximum	First Quartile	Second Quartile	Third Quartile	P-value
Orbital face height L	**en' L - gn'**	**212**	**110.131**	**5.846**	**94.032**	**128.203**	**105.754**	**109.370**	**113.834**	**0.099**
Orbital face height R	en' R - gn'	212	110.209	5.778	95.894	129.085	105.859	109.627	114.130	0.200
Face height	n' - gn'	212	117.297	6.617	100.476	138.979	112.605	116.852	121.651	0.063
Upper face height	n' - sto'	215	77.032	4.557	66.124	87.879	73.871	76.913	80.062	0.200
Lower face depth L	obi' L - gn'	211	128.057	6.262	112.545	143.088	123.756	128.286	132.948	0.200
Lower face depth R	obi' R - gn'	211	129.313	6.581	112.071	148.784	124.462	130.295	133.912	0.025
Mid-face depth L	obi' L - sn'	214	121.599	4.955	110.178	134.422	118.161	121.067	125.355	0.200
Mid-face depth R	obi' R - sn'	214	122.355	5.489	109.217	139.763	118.669	121.867	126.417	0.200
Lower chin height	pg' - gn'	178	8.295	2.001	4.348	18.015	7.055	8.072	9.353	**0.001***
Chin height	sm' - gn'	207	21.984	3.177	13.479	34.387	19.870	21.791	23.702	0.017
Lower face height	sn' - gn'	212	62.524	5.023	48.814	80.237	58.867	62.217	65.979	0.200
Mandible height	sto' - gn'	212	40.793	3.603	32.736	53.885	38.163	40.760	42.756	0.200
Intercanthal width	en' – en'	215	33.795	2.801	26.422	41.871	31.634	33.900	35.911	0.200
Eye fissure width L	ex' L - en' L	215	30.939	2.886	21.076	41.986	29.067	30.584	32.526	0.078
Eye fissure width R	ex' R - en' R	215	31.642	2.771	24.414	40.512	29.574	31.386	33.018	**0.002***
Biocular width	ex' – ex'	215	93.975	5.122	79.820	108.503	90.624	93.481	97.359	0.087
Nose width	al' – al'	215	35.642	2.465	30.727	43.756	33.708	35.454	37.298	0.200
Nasal bridge length	n' - prn'	215	48.948	3.877	35.842	57.884	46.114	48.840	51.518	0.200
Nose height	n' - sn'	215	56.175	3.726	46.950	66.183	53.946	56.025	58.849	0.200
Nasal tip protrusion	sn' - prn'	215	21.779	2.183	16.162	28.865	20.271	21.872	23.139	0.200
Mouth width	ch' – ch'	215	50.904	3.832	38.422	62.440	48.535	50.643	53.407	0.200
Half mouth width L	ch' L - sto'	215	28.210	2.806	20.212	41.533	26.238	28.142	29.947	0.200
Half mouth width R	ch' R - sto'	215	28.586	2.646	20.759	35.740	27.031	28.559	30.268	0.200
Upper vermillion height	ls' - sto'	215	9.052	2.490	1.748	15.398	7.663	9.160	10.662	0.200
Lower vermillion height	li' - sto'	215	9.269	2.584	1.598	14.798	7.637	9.527	11.036	0.047
Distance mso-gn L	mso' L - gn'	212	126.161	6.481	107.700	147.373	121.799	125.397	130.493	0.023
Distance mso-gn R	mso' R - gn'	212	126.110	6.562	108.030	146.687	121.525	125.418	130.550	0.042

*Kolmogorov-Smirnov test significant at P-value <0.01, indicating that the morphofacial variables do not follow a normal distribution.

Table 7. Basic statistics of Spanish male anthropometric indices and P-values for Kolmogorov-Smirnov test.

Anthropometric linear measurements	Abv	Descriptive								Kolmogorov-Smirnov
		N	Mean	SD	Minimun	Maximum	First Quartile	Second Quartile	Third Quartile	P-value
Intercanthal index	en' - en' / ex' - ex' x 100	215	35.995	2.735	29.137	44.525	34.212	36.095	37.865	0.200
Nose-face height index	n' - sn' / n '- gn' x 100	212	47.921	2.511	40.947	53.891	46.285	48.035	49.654	0.200
Nasal index	al' - al' / n' - sn' x 100	215	63.733	6.172	49.904	79.670	59.665	62.876	67.481	0.025
Intercanthal-nasal width index	en' - en' / al' - al' x 100	215	95.141	8.950	74.556	115.627	89.604	95.485	101.609	0.200
Nose-mouth width index	al' - al' / ch'- ch' x 100	215	70.294	5.882	58.516	94.297	65.390	70.031	74.168	0.023
Upper face-face height index	n' - sto' / n' - gn' x 100	212	65.680	2.054	57.557	72.132	64.408	65.618	66.983	0.200
Mandibulo-face height index	sto' - gn '/ n' - gn' x 100	212	34.760	2.062	28.241	42.450	33.405	34.751	36.011	0.200
Mandibulo-upper face height index	sto' - gn' / n' - sto' x 100	212	53.072	4.811	39.236	73.753	49.835	52.888	55.811	0.200
Mandibulo-lower face height Index	sto' - gn' / sn' - gn' x 100	212	65.270	2.924	57.416	73.459	63.478	65.264	67.336	0.200
Orbital width index L	ex' L - en' L / en' - en' x 100	215	92.205	11.696	55.929	130.792	83.985	91.342	97.970	0.011
Orbital width index R	ex' R - en' R / en' - en' x 100	215	94.321	11.808	66.418	128.523	85.680	92.657	101.102	0.031
Nasal tip protrusion-width index	sn' - prn' / al' - al' x 100	215	61.340	7.041	43.162	86.300	56.280	60.558	65.855	0.200
Nasal tip protrusion-height index	sn' - prn' / n' - sn' x 100	215	38.822	3.533	30.180	48.278	36.578	39.018	41.099	0.200
Upper lip height-mouth index	sn' - sto' / ch' - ch' x 100	215	43.403	5.860	26.679	58.169	39.573	43.056	47.349	0.200
Vermilion height index	ls' - sto' / sto' - li' x 100	215	100.508	24.200	59.161	249.737	84.193	96.925	112.710	**0.000***
Nasal bridge index	n' - prn' / n' - sn' x 100	215	87.140	3.934	76.342	102.609	84.990	87.250	89.467	0.200
Upper face height-biocular width index	n' - sto' / ex' - ex' x 100	215	82.170	6.077	68.336	100.363	77.797	81.861	86.056	0.200
Intercanthal width-upper face height index	en' - en' / n' - sto' x 100	215	44.009	4.337	33.888	57.388	41.258	43.719	46.678	0.200
Intercanthal-mouth width index	en' - en' / ch' - ch' x 100	215	66.723	7.230	49.573	99.561	61.265	65.809	71.557	0.025
Upper lip-face height index	sn' - sto' / sn' - gn' x 100	212	35.120	2.972	27.871	45.348	33.055	35.252	36.792	0.200
Lower lip-face height index	sto' - sm' / sn' - gn' x 100	207	30.706	3.333	17.201	38.192	28.952	31.053	32.758	0.025

Table 8. Basic statistics of Spanish female anthropometric linear measurements and P-values for Kolmogorov-Smirnov test.

Anthropometric linear measurements	Abv	Descriptive statistics								Kolmogorov-Smirnov
		N	Mean	SD	Mini-mun	Maxi-mum	First Quartile	Second Quartile	Third Quartile	P-value
Orbital face height L	en' L - gn'	319	101.131	5.168	88.010	121.418	97.825	100.654	104.438	0.200
Orbital face height R	en' R - gn'	318	101.344	5.195	88.757	123.877	97.833	101.178	104.771	0.200
Face height	n' - gn'	319	110.679	6.090	92.173	132.260	106.718	110.405	114.733	0.200
Upper face height	n' - sto'	320	73.885	4.390	61.264	86.173	70.958	73.693	76.905	0.200
Lower face depth L	obi' L - gn'	312	117.922	6.000	92.277	135.109	114.227	117.945	121.692	0.200
Lower face depth R	obi' R - gn'	312	118.826	5.977	91.908	135.727	114.805	119.227	122.641	0.200
Mid-face depth L	obi' L - sn'	313	113.346	4.790	100.629	125.755	109.767	113.457	116.237	0.200
Mid-face depth R	obi' R - sn'	313	113.565	4.915	97.838	127.078	110.044	113.575	116.724	0.200
Lower chin height	pg' - gn'	251	7.344	1.372	4.554	13.961	6.359	7.224	8.115	0.200
Chin height	sm' - gn'	319	19.952	2.521	12.770	30.032	18.170	19.890	21.684	0.200
Lower face height	sn' - gn'	319	57.186	4.502	45.696	72.834	54.586	56.927	59.994	0.200
Mandible height	sto' - gn'	319	37.296	3.159	28.642	48.976	35.270	37.223	39.502	0.200
Intercanthal width	en' – en'	319	31.805	2.413	25.568	39.395	30.186	31.759	33.263	0.096
Eye fissure width L	ex' L - en' L	320	30.242	2.767	23.623	39.229	28.321	30.021	32.217	0.092
Eye fissure width R	ex' R - en' R	319	30.577	2.596	22.881	38.471	28.658	30.499	32.227	0.200
Biocular width	ex' – ex'	320	90.295	4.486	78.940	103.198	87.378	90.499	93.165	0.200
Nose width	al' – al'	320	32.264	2.262	26.679	38.951	30.670	32.049	33.773	0.060
Nasal bridge length	n' - prn'	320	47.328	3.848	36.214	61.019	44.835	47.110	49.727	0.086
Nose height	n' - sn'	320	54.732	3.483	43.756	65.329	52.770	54.520	56.801	0.043
Nasal tip protrusion	sn' - prn'	320	20.976	1.859	16.447	25.573	19.709	20.907	22.183	0.066
Mouth width	ch' – ch'	320	48.216	3.217	38.301	57.838	45.965	48.065	50.202	0.200
Half mouth width L	ch' L - sto'	320	26.896	2.221	19.890	33.779	25.360	26.763	28.171	0.200
Half mouth width R	ch' R - sto'	320	27.096	2.377	20.175	35.309	25.502	26.996	28.656	0.200
Upper vermillion height	ls' - sto'	320	8.828	2.045	3.378	16.105	7.705	8.763	9.981	**0.003***
Lower vermillion height	li' - sto'	320	9.342	2.081	3.477	14.943	7.982	9.366	10.915	0.200
Distance mso-gn L	mso' L - gn'	319	120.173	5.987	103.475	141.921	116.110	119.858	124.222	0.200
Distance mso-gn R	mso' R - gn'	319	120.259	6.054	105.180	145.140	116.150	120.252	124.386	0.200

*Kolmogorov-Smirnov test significant at P-value <0.01, indicating that the morphofacial variables do not follow a normal distribution.

Table 9. Basic statistics of Spanish female anthropometric indices and P-values for Kolmogorov-Smirnov test.

Anthropometric indices	Abv	Descriptive statistics								Kolmogorov-Smirnov
		N	Mean	SD	Min.	Max.	First Quartile	Second Quartile	Third Quartile	P-value
Intercanthal index	en' - en' / ex' - ex' x 100	319	35.270	2.687	28.138	43.832	33.649	35.489	36.997	0.051
Nose-face height index	n' - sn' / n '- gn' x 100	319	49.481	2.235	43.305	55.685	47.957	49.440	50.874	0.200
Nasal index	al' - al' / n' - sn' x 100	320	59.188	5.640	46.233	78.580	55.283	58.608	62.697	**0.008***
Intercanthal-nasal width index	en' - en' / al' - al' x 100	319	98.935	8.766	75.782	127.486	92.802	99.114	104.495	0.200
Nose-mouth width index	al' - al' / ch'- ch' x 100	320	67.087	5.020	54.947	81.672	63.341	66.748	70.526	0.200
Upper face-face height index	n' - sto' / n' - gn' x 100	319	66.772	1.919	61.741	71.862	65.456	66.632	68.171	0.200
Mandibulo-face height index	sto' - gn '/ n' - gn' x 100	319	33.683	1.937	28.174	39.142	32.265	33.750	35.013	0.200
Mandibulo-upper face height index	sto' - gn' / n' - sto' x 100	319	50.567	4.322	39.206	63.398	47.272	50.628	53.553	0.200
Mandibulo-lower face height Index	sto' - gn' / sn' - gn' x 100	319	65.249	2.899	56.835	72.435	63.119	65.406	67.400	0.200
Orbital width index L	ex' L - en' L / en' - en' x 100	319	95.766	12.640	66.767	145.610	87.125	93.486	103.467	**0.000***
Orbital width index R	ex' R - en' R / en' - en' x 100	319	96.808	12.144	64.840	133.830	88.639	95.342	104.196	**0.000***
Nasal tip protrusion-width index	sn' - prn' / al' - al' x 100	320	65.304	7.147	48.912	89.935	60.203	65.142	70.036	0.200
Nasal tip protrusion-height index	sn' - prn' / n' - sn' x 100	320	38.424	3.645	29.628	50.513	36.055	38.294	40.522	0.093
Upper lip height-mouth index	sn' - sto' / ch' - ch' x 100	320	41.865	5.538	26.175	63.247	38.171	41.520	45.148	0.099
Vermilion height index	ls' - sto' / sto' - li' x 100	320	96.350	20.065	49.159	183.035	82.252	95.401	107.072	0.015
Nasal bridge index	n' - prn' / n' - sn' x 100	320	86.434	3.456	74.646	96.296	84.555	86.702	88.523	0.031
Upper face height-biocular width index	n' - sto' / ex' - ex' x 100	320	82.003	6.038	67.020	104.633	77.742	81.996	85.915	0.200
Intercanthal width-upper face height index	en' - en' / n' - sto' x 100	319	43.203	4.229	33.080	54.279	40.300	42.891	45.572	0.014
Intercanthal-mouth width index	en' - en' / ch' - ch' x 100	319	66.227	6.084	49.899	84.608	62.470	66.411	70.200	0.200
Upper lip-face height index	sn' - sto' / sn' - gn' x 100	319	35.145	2.965	27.618	43.558	32.964	35.018	37.399	0.200
Lower lip-face height index	sto' - sm' / sn' - gn' x 100	319	30.759	3.196	16.457	40.110	28.753	30.858	32.874	**0.007***

* Kolmogorov-Smirnov test significant at P-value <0.01, indicating that the morphofacial variables do not follow a normal distribution.

Table 10. Results after comparison analysis between male and female linear measurements and association analysis with BMI. P-values <0.001 are highlighted in bold.

Anthropometric linear measurements	Abv	Comparison Male-Female	Correlation BMI	
		P-value	Correlation coefficient	P-value
Orbital face height L	en' L - gn'	**0.000****	-0.005	0.908
Orbital face height R	en' R - gn'	**0.000****	-0.013	0.758
Face height	n' - gn'	**0.000****	-0.007	0.878
Upper face height	n' - sto'	**0.000****	-0.007	0.878
Lower face depth L	obi' L - gn'	**0.000****	-0.093	0.035
Lower face depth R	obi' R - gn'	**0.000****	**0.382**[a]	**0.000****
Mid-face depth L	obi' L - sn'	**0.000****	**-0.160**[a]	**0.000****
Mid-face depth R	obi' R - sn'	**0.000****	**-0.143**[a]	**0.001***
Lower chin height	pg' - gn'	**0.000****	**0.201**[a]	**0.000****
Chin height	sm' - gn'	**0.000****	**0.244**[a]	**0.000****
Lower face height	sn' - gn'	**0.000****	0.004	0.927
Mandible height	sto' - gn'	**0.000****	0.009	0.838
Intercanthal width	en' – en'	**0.000****	-0.084	0.053
Eye fissure width L	ex' L - en' L	**0.003***	0.011	0.793
Eye fissure width R	ex' R - en' R	**0.000****	0.093	0.032
Biocular width	ex' – ex'	**0.000****	-0.039	0.373
Nose width	al' – al'	**0.000****	-0.051	0.245
Nasal bridge length	n' - prn'	**0.000****	-0.053	0.222
Nose height	n' - sn'	**0.000****	-0.020	0.652
Nasal tip protrusion	sn' - prn'	**0.000****	0.009	0.829
Mouth width	ch' – ch'	**0.000****	-0.005	0.910
Half mouth width L	ch' L - sto'	**0.000****	0.006	0.891
Half mouth width R	ch' R - sto'	**0.000****	0.001	0.974
Upper vermillion height	ls' - sto'	0.136	-0.111	0.010
Lower vermillion height	li' - sto'	0.865	-0.108	0.013
Distance mso-gn L	mso' L - gn'	**0.000****	**0.14**[a]	**0.001***
Distance mso-gn R	mso' R - gn'	**0.000****	**0.145**[a]	**0.001****

*P-values <0.01 | ** P-values <0.001 | [a] Weak correlation

Table 11. Results after comparison analysis between male and female indices and association analysis with BMI. P-values <0.001 are highlighted in bold.

Anthropometric linear measurements	Abv	Comparison Male-Female	Correlation BMI	
		P-value	Correlation coefficient	P-value
Intercanthal index	en' - en' / ex' - ex' x 100	**0.001***	-0.064	0.141
Nose-face height index	n' - sn' / n '- gn' x 100	**0.000****	-0.049	0.259
Nasal index	al' - al' / n' - sn' x 100	**0.000****	**0.216** [a]	**0.000****
Intercanthal-nasal width index	en' - en' / al' - al' x 100	**0.000****	-0.033	0.443
Nose-mouth width index	al' - al' / ch'- ch' x 100	**0.000****	-0.046	0.292
Upper face-face height index	n' - sto' / n' - gn' x 100	**0.000****	-0.032	0.469
Mandibulo-face height index	sto' - gn '/ n' - gn' x 100	**0.000****	0.023	0.596
Mandibulo-upper face height index	sto' - gn' / n' - sto' x 100	**0.000****	0.024	0.586
Mandibulo-lower face height Index	sto' - gn' / sn' - gn' x 100	0.468	0.016	0.715
Orbital width index L	ex' L - en' L / en' - en' x 100	**0.004***	-0.028	0.528
Orbital width index R	ex' R - en' R / en' - en' x 100	0.016	-0.013	0.766
Nasal tip protrusion-width index	sn' - prn' / al' - al' x 100	**0.000****	0.044	0.310
Nasal tip protrusion-height index	sn' - prn' / n' - sn' x 100	0.105	0.040	0.359
Upper lip height-mouth index	sn' - sto' / ch' - ch' x 100	**0.001***	-0.010	0.813
Vermilion height index	ls' - sto' / sto' - li' x 100	0.115	0.013	0.765
Nasal bridge index	n' - prn' / n' - sn' x 100	0.045	-0.096	0.028
Upper face height-biocular width index	n' - sto' / ex' - ex' x 100	0.861	-0.046	0.290
Intercanthal width-upper face height index	en' - en' / n' - sto' x 100	0.017	0.052	0.232
Intercanthal-mouth width index	en' - en' / ch' - ch' x 100	0.904	-0.015	0.724
Upper lip-face height index	sn' - sto' / sn' - gn' x 100	0.462	-0.025	0.565
Lower lip-face height index	sto' - sm' / sn' - gn' x 100	0.897	**-0.182** [a]	**0.000****

*P-values <0.01 | ** P-values <0.001 | [a] Weak correlation

Table 12. Results after comparison analysis of linear measurements between young and middle/older age groups. P-values <0.001 are highlighted in bold.

Anthropometric measurements and indices	Abv	Comparison Young -Middle/Older	Comparison Young -Middle/Older MALE	Comparison Young -Middle/Older FEMALE
		P-value	*P-value*	*P-value*
Orbital face height L	en L - gn	**0.001****	**0.001***	**0.000****
Orbital face height R	en R - gn	**0.001***	**0.003***	**0.000****
Face height	n - gn	**0.001***	**0.002***	0.010
Upper face height	n - sto	**0.000****	**0.000****	**0.000****
Lower face depth L	obi L - gn	0.222	0.036	0.212
Lower face depth R	obi R - gn	0.081	0.030	0.056
Mid-face depth L	obi L - sn	0.824	0.286	0.817
Mid-face depth R	obi R - sn	0.393	0.121	0.488
Lower chin height	pg - gn	0.304	0.944	0.355
Chin height	sm - gn	0.471	0.955	0.444
Lower face height	sn - gn	0.142	0.140	0.133
Mandible height	sto - gn	0.083	0.594	0.101
Intercanthal width	en – en	0.505	0.197	0.561
Eye fissure width L	ex L - en L	**0.007***	0.441	**0.005***
Eye fissure width R	ex R - en R	**0.007***	0.637	**0.001***
Biocular width	ex – ex	0.022	0.547	0.013
Nose width	al – al	**0.000****	**0.001****	**0.000****
Nasal bridge length	n - prn	**0.000****	**0.000****	**0.006***
Nose height	n - sn	**0.004***	**0.005***	0.109
Nasal tip protrusion	sn - prn	**0.000****	**0.000****	**0.000****
Mouth width	ch – ch	0.029	0.391	**0.006***
Half mouth width L	ch L - sto	**0.000****	**0.000****	**0.000****
Half mouth width R	ch R - sto	**0.007***	0.529	**0.001****
Upper vermillion height	ls - sto	**0.000****	**0.000****	**0.000****
Lower vermillion height	li - sto	**0.000****	**0.000****	**0.000****
Distance mso-gn L	mso L - gn	0.128	0.054	0.300
Distance mso-gn R	mso R - gn	0.099	0.067	0.203

*P-values <0.01 | ** P-values <0.001

Table 13. Results after comparison analysis of indices between young and middle/older age groups. P-values <0.001 are highlighted in bold.

Anthropometric measurements and indices	Abv	Comparison Young -Middle/Older	Comparison Young -Middle/Older MALE	Comparison Young -Middle/Older FEMALE
		P-value	*P-value*	*P-value*
Intercanthal index	en - en / ex - ex x 100	0.300	0.388	0.023
Nose-face height index	n - sn / n - gn x 100	0.819	0.860	0.419
Nasal index	al - al / n - sn x 100	0.327	0.669	0.172
Intercanthal-nasal width index	en - en / al - al x 100	**0.000****	**0.000****	0.020
Nose-mouth width index	al - al / ch - ch x 100	0.048	0.033	0.294
Upper face-face height index	n - sto / n - gn x 100	**0.000****	**0.000****	**0.000****
Mandibulo-face height index	sto - gn / n - gn x 100	**0.000****	**0.000****	**0.000****
Mandibulo-upper face height index	sto - gn / n - sto x 100	**0.000****	**0.000****	**0.000****
Mandibulo-lower face height Index	sto - gn / sn - gn x 100	**0.000****	**0.000****	**0.000****
Orbital width index L	ex L - en L / en - en x 100	0.171	0.607	0.020
Orbital width index R	ex R - en R / en - en x 100	0.169	0.293	0.016
Nasal tip protrusion-width index	sn - prn / al - al x 100	0.021	0.302	0.043
Nasal tip protrusion-height index	sn - prn / n - sn x 100	**0.000****	0.061	**0.000****
Upper lip height-mouth index	sn - sto / ch - ch x 100	**0.000****	**0.007***	**0.003***
Vermilion height index	ls - sto / sto - li x 100	0.288	0.101	0.964
Nasal bridge index	n - prn / n - sn x 100	**0.001****	0.060	**0.003***
Upper face height-biocular width index	n - sto / ex - ex x 100	**0.000****	**0.000****	**0.000****
Intercanthal width-upper face height index	en - en / n - sto x 100	**0.000****	**0.000****	**0.028**
Intercanthal-mouth width index	en - en / ch - ch x 100	0.038	0.143	0.149
Upper lip-face height index	sn - sto / sn - gn x 100	**0.000****	**0.000****	**0.000****
Lower lip-face height index	sto - sm / sn - gn x 100	**0.003***	0.039	0.014

*P-values <0.01 | ** P-values <0.001

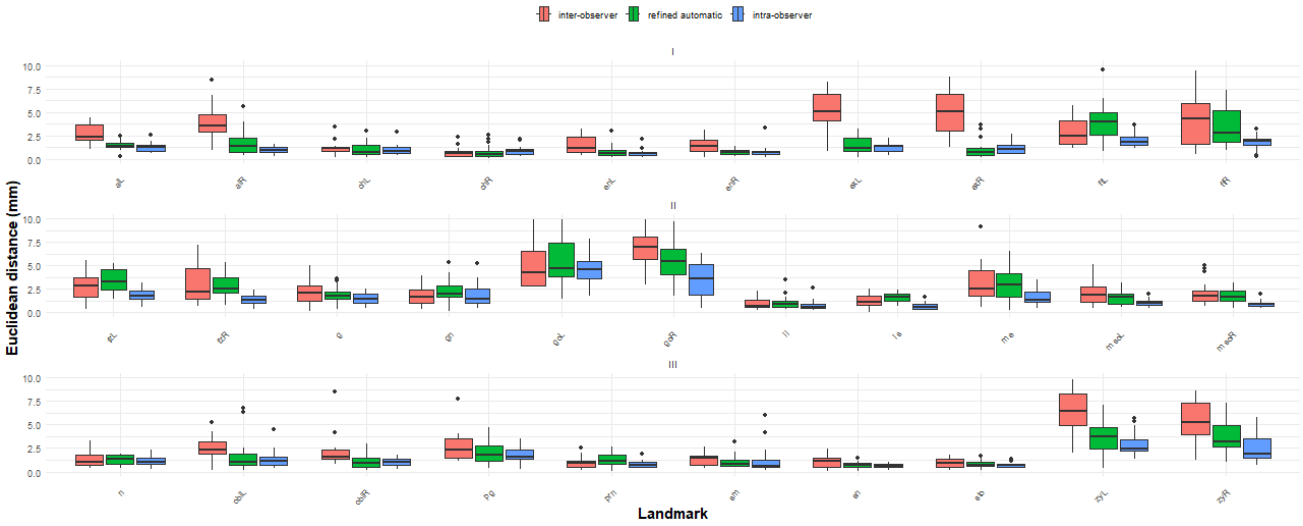

Supplementary Fig. S1.- Boxplots showing the dispersion analysis of cephalometric landmark localization across 31 landmarks, comparing the inter-observer, the intra-observer, and the refined automatic method.

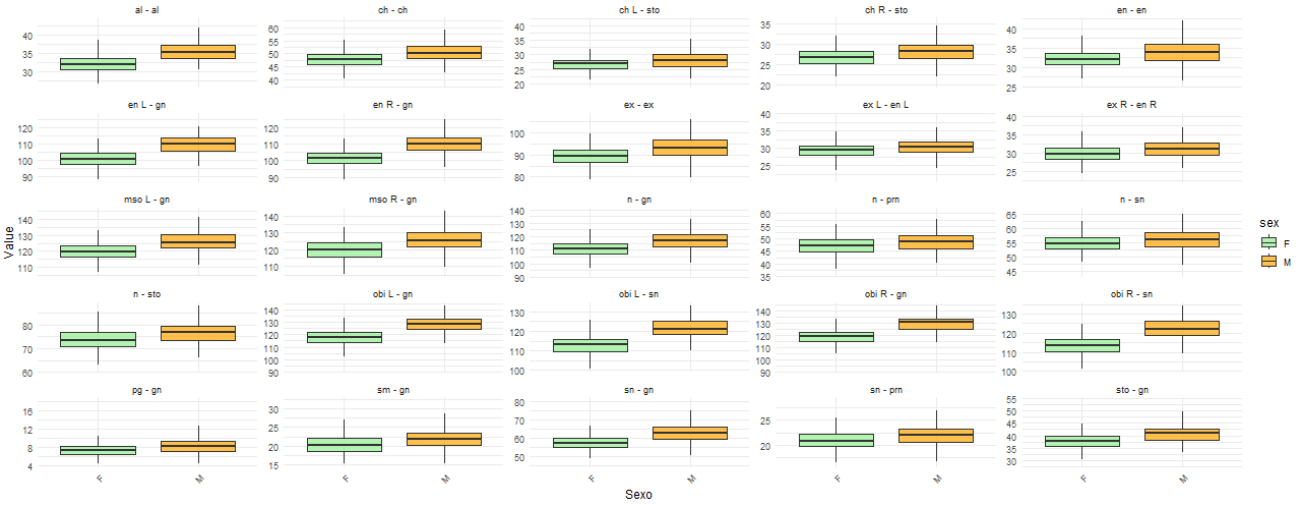

Supplementary Fig. S2.- Boxplots comparing various anthropometric linear measurements with statistically significant differences between males (M) and females (F).

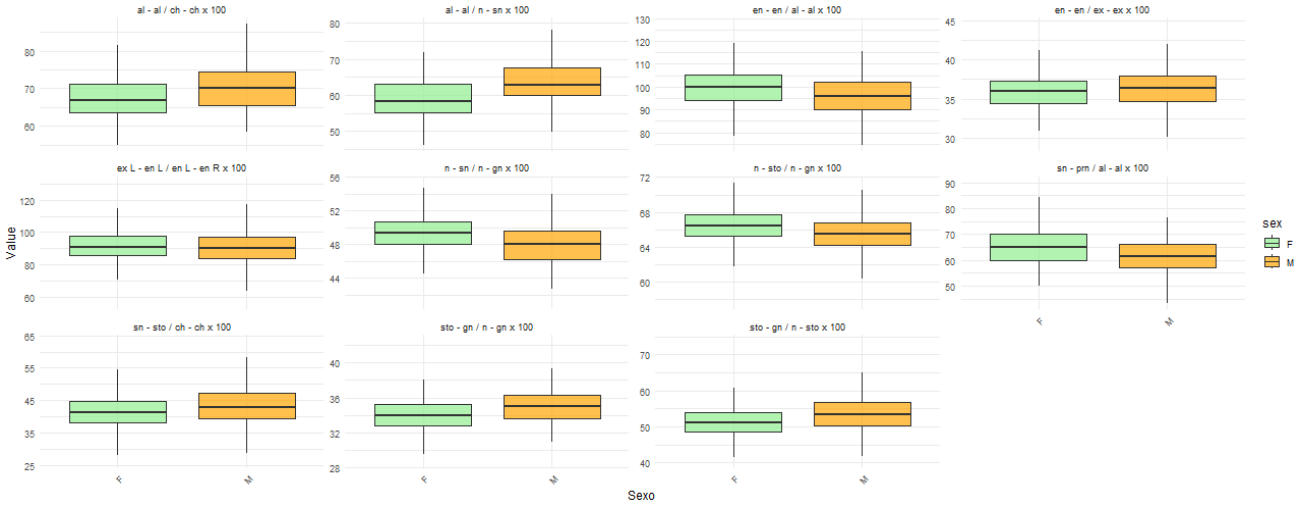

Supplementary Fig. S3.- Boxplots comparing various anthropometric indices with statistically significant differences between males (M) and females (F).

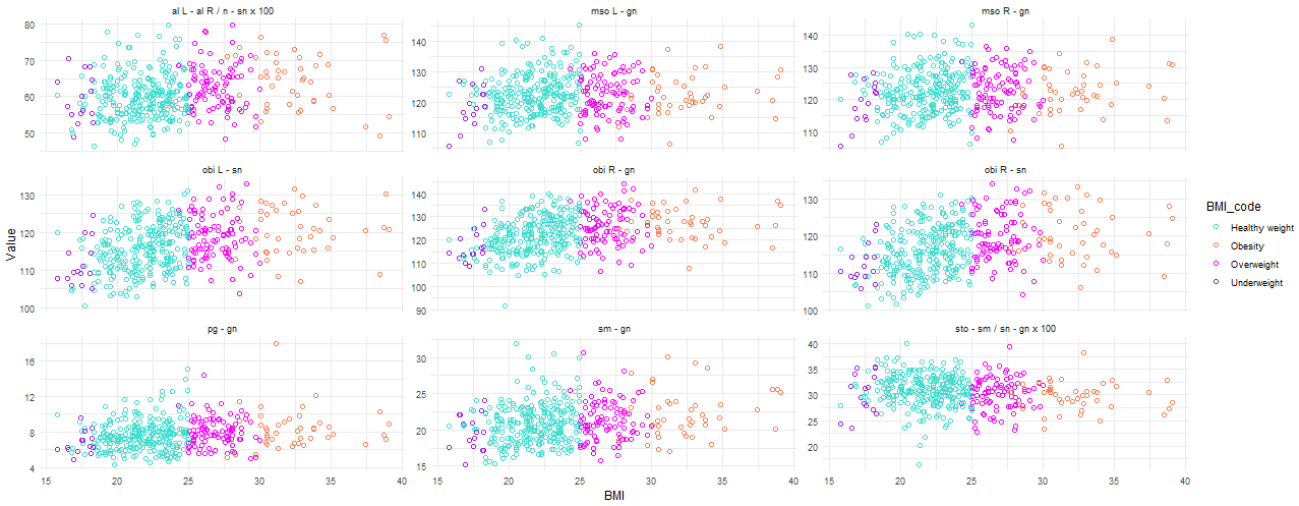

Supplementary Fig. S4.- Scatter plots of the linear measurements and proportionality indices showing a correlation with BMI.

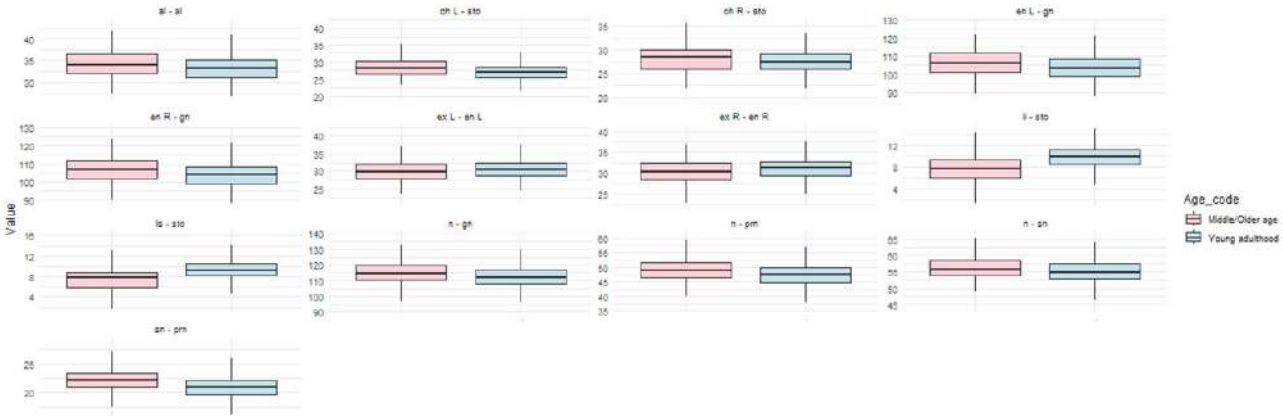

Supplementary Fig. S5.- Boxplots comparing various anthropometric linear measurements with statistically significant differences between young adulthood and middle/older age groups.

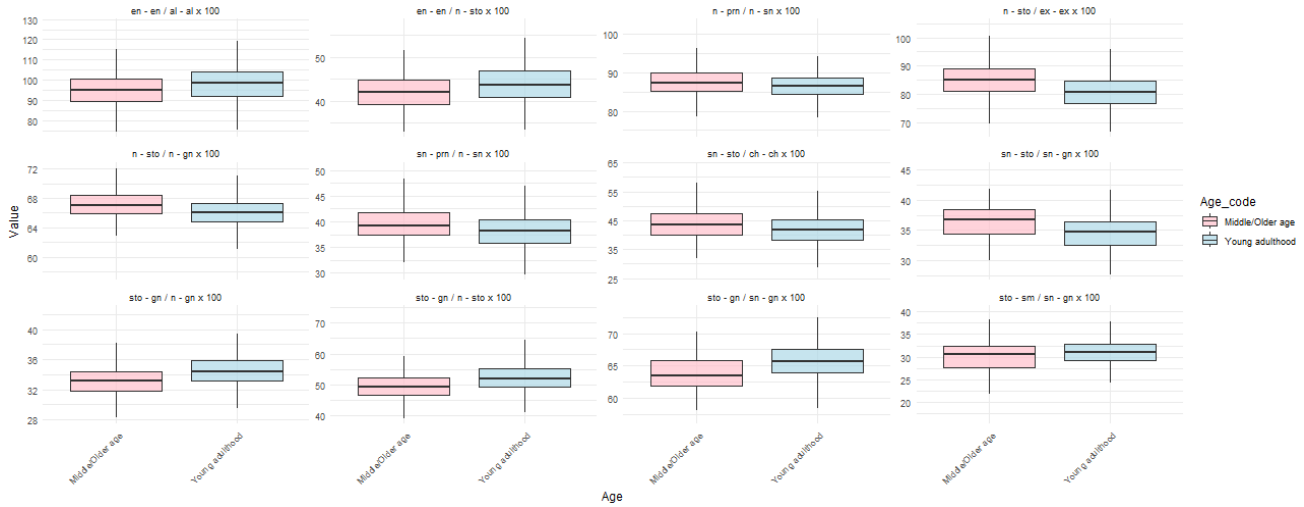

Supplementary Fig. S6.- Boxplots comparing various anthropometric indices with statistically significant differences between young adulthood and middle/older age groups.

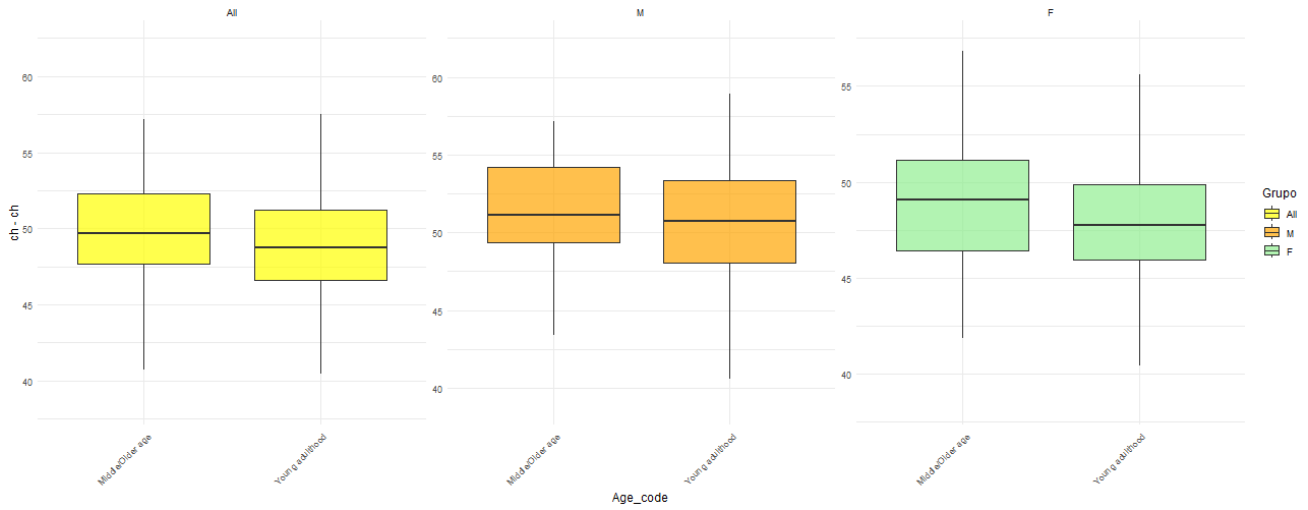

Supplementary Fig. S7.- Boxplots comparing mouth width (ch – ch), showing statistically significant differences between age groups exclusively in females. "All" represents males and females combined, "M" represents males, and "F" represents females.

ric data from one population group to individuals from a different group can lead to inaccuracies and misdiagnosis, particularly when relying on neoclassical canons for comparison (Farkas, 1996; Farkas et al., 2000). This variability in facial morphology among populations highlights the challenge clinicians face in distinguishing between normal and abnormal features in a patient's face. Factors such as age, sex and ancestry introduce a significant number of variables, necessitating population-specific reference data for accurate diagnosis and treatment.

Previous studies, such as those by Farkas and others, have revealed substantial differences between intercontinental populations and the neoclassical canons often used in facial analysis (Farkas, 1994; Farkas et al., 1985; Farkas et al., 2000; Farkas and Cheung, 1981; Kim, 2017). Various population groups, including Indian (Jagadish Chandra et al., 2012), Iranian (Jahanshahi et al., 2008), Turkish (Borman et al., 1999), Chinese (Dong et al., 2011), Korean (Baik et al., 2007), Kenyan-African (Virdi et al., 2019), have exhibited distinct facial traits, further emphasizing the need for establishing specific normative anthropometric data for each group.

In this study, we utilized a contemporary non-invasive 3D photo anthropometric method to analyze the facial features of healthy adults with neutral expression from different regions of Spain. This allowed us to establish anthropometric reference values for soft tissue facial features within this specific population. Furthermore, we investigated potential sex-based differences within this population.

Previous studies have reported variations in Southern Spanish population (50 males and 50 females) head and facial shapes for orthodontic diagnosis employing a 3D photography device (Menéndez López-Mateos et al., 2019). Although these results may provide insights into standard sizes and variations in the population under study, the sample used is limited to a single region in southern Spain. Thus, in this study, we established an extensive set of standard reference data for the Spanish population, employing a 3D capture system and 3D digital imaging technologies. This effort yielded fundamental statistics, including mean values, standard deviations, minimum and maximum values, as well as the first, second, and third quartiles, for 21 anthropometric linear measurements and 20 indices across 535 individuals.

To locate the 31 landmarks necessary for estimating anthropometric measurements and indices in the 535 facial 3D models, the automatic template fitting method described in (Bermejo et al., 2021) has been employed. This method provides a complete initialization of the landmark coordinates, significantly reducing the time re-

quired by experts to process large volumes of data efficiently. The findings indicate that the localization errors of cephalometric landmarks obtained through the refinement method (2.170 mm) are consistent with those reported in existing literature, with average errors ranging between 1.88 and 2.51 mm (Bermejo et al., 2021; Gupta et al., 2015; Montúfar et al., 2018; Neelapu et al., 2018). Although our results align closely with these figures, direct comparison between methods is not feasible. This limitation arises from the influence of the specific set of landmarks studied in each method, which significantly impacts the final magnitude of the localization error.

The comparison of linear measurements and indices of the face revealed significant differences between males and females' subjects in most facial variables that were analyzed.

A pronounced sexual dimorphism was observed, with statistically significant differences in 25 of the 27 linear measurements under study. These results, with significant differences observed in nearly all measures and with males showing higher values, align with previous studies (Othman et al., 2016; Ozdemir et al., 2009). Similarly, the lack of significant differences in the upper and lower vermilion height is also in consonance with the findings of Ozdemir et al. (2009) and Othman et al. (2016).

For the indices, only 11 of the 21 studied showed significant differences. Among the results observed, the differences found for the intercanthal-nasal width index were also reported in Menéndez López-Mateos et al. (2019), with this index being higher in females than in males in both studies. Despite not having examined the same indices (only one in common), in general the lower proportion of indices with significant differences compared to the proportion of measures is recurrent and consistent between the two analyses.

However, our findings do not align with previous studies using quasi-landmarks in individuals of European ancestry, which suggest sexual dimorphism with more prominent forward projection in males and broader, flatter faces in females (Bannister et al., 2022; Matthews et al., 2018, 2023). While our results show males have wider and higher faces, this contrasts with mesh-based studies, where female faces were broader. These discrepancies may be attributed to allometric differences between sexes. Future research should account for these differences to assess whether shape, rather than size, distinctions exist between males and females in the Spanish population

The correlation analysis between BMI and various facial measures and indices revealed nine statistically significant weak correlations. These results are consistent with prior studies on facial morphology, which have identified BMI as a contributing factor to variations in transverse dimensions (Rongo et al., 2014). Previous investigations have also highlighted an association between increased BMI and broader faces, along with the impact of BMI on lower facial width, echoing observations in the present study (Coetzee et al., 2010; Geniole et al., 2015; Mayew, 2013; Pham et al., 2011; Skomina et al., 2020). Moreover, our results align with the localized distribution of facial fat, primarily in the buccal fat pads situated in the cheek (Kahn et al., 2000; Tostevin and Ellis, 1995).

The comparison of measurements and indices between young and middle/older adulthood individuals revealed statistically significant differences in more than half of the variables under study, primarily affecting the eyes, nose, mouth, and mandible.

Age-related increases in muscular and ligamentous laxity, combined with bone density loss, contribute to the progressive descent of adipose and soft tissue in specific facial regions (Kaur et al., 2015). The alterations in the periorbital contour here observed align with previous findings from diverse populations (Imaizumi et al., 2015; Lee et al., 2019; Liu et al., 2023; Velemínská et al., 2022). Notably, Sforza et al. documented a progressive inferior displacement of the orbitale landmark with age (Sforza et al., 2009). Changes in the nasal region are consistent with those reported by Velemínská et al. and of Sforza et al., both of whom described an age-related increase in nasal length and width (Sforza et al., 2009; Velemínská et al., 2022). Similarly, variations in lip morphology align with prior studies which identified age-associated lip flattening (Imaizumi et al., 2015; Lee

et al., 2019; Sforza et al., 2009; Velemínská et al., 2022).

Interestingly, sex-specific differences in age-related facial changes were identified. Our findings suggest that in females the most specific aging changes occur in mouth width.

One limitation of this study is that the analyzed sample does not include children or adolescents, focusing exclusively on the adult population. Expanding this research to cover the entire range of variation within the Spanish population, including different age groups, would provide valuable insights into ontogenetic changes in facial morphology. Understanding how facial shape evolves over the course of life could contribute to improving forensic age estimation, orthodontic and surgical planning, and anthropological studies. Future research should aim to analyze facial growth patterns and age-related morphological changes using the same 3D photoanthropometric methodology to establish a comprehensive database that captures the full spectrum of facial variation in Spain.

Additionally, recent studies have suggested the potential use of facial biomarkers for the diagnosis and prognosis of genetic, rare, and psychotic disorders (Echeverry-Quiceno et al., 2023; Gurovich et al., 2018; Hallgrímsson et al., 2020; Heredia-Lidón et al., 2024). Facial morphology can serve as a diagnostic tool in various medical fields, offering insights into conditions with craniofacial manifestations. The application of 3D photoanthropometry in medical diagnostics is a promising area for future research, as it may contribute to the early detection and personalized treatment of such disorders. Expanding our database to include facial variation associated with specific conditions could further enhance the clinical applicability of this approach.

Looking toward future perspectives, as previously discussed, the data collected using traditional measurements and indices can serve as a valuable database for the quantitative description of human facial morphology within a population. Furthermore, given that this traditional approach has been widely used by anthropologists, there exists a substantial amount of data for certain measurements and indices across different populations. However, integrating emerging techniques, such as utilizing quasi-landmark meshes, could offer significant value by providing additional insights into the effects of variables such as sex, age, BMI, and size on facial morphology. These methods not only capture size information but also provide a detailed understanding of the directional shape of facial regions. Expanding and complementing the existing reference data based on traditional landmarks with these novel approaches could represent the next step in conducting the most comprehensive anthropological analysis of the Spanish population.

Conclusions

This study provides valuable insights into the facial anthropometry of the Spanish population using non-invasive 3D photoanthropometry. The comparison of linear measurements and indices revealed significant sexual dimorphism, with males generally exhibiting higher values across most facial variables analyzed. These findings corroborate previous research and underscore the importance of considering sex-specific differences in facial morphology assessment. Additionally, our analysis of indices showed a lower proportion of significant differences compared to linear measurements, consistent with previous studies. Considering the BMI, we have found a weak correlations with the lower facial region, in line with prior studies. Age-related differences were also observed, with certain variations consistently appearing in both sexes, while others were specific to females. Overall, these results contribute to the establishment of reference anthropometric data for the Spanish adult population, representing a significant advancement within this demographic context. Moreover, they highlight the necessity of tailored approaches in facial morphological studies to ensure accurate and applicable results.

ACKNOWLEDGEMENTS

This research has been developed within the RandD project CONFIA (grant PID2021-122916NB-I00), funded by MICIU/AEI/10.13039/5011000 11033/ and by EDRF/EU. Authors also acknowledge funding support from Basque Government under predoctoral fellowship PRE_2021_2_0157 to Belén Navarro. Victoria Suárez-

Ulloa is partner and researcher at Panacea Cooperative Research. Her work in this project was funded by a grant Torres Quevedo PTQ2022-012683. Identities of volunteer data donors were not accessible to Panacea or any researcher involved following approved protocols by the ethical committee of University of the Basque Country UPV/EHU M10/2021/143. The authors are grateful to the entire CIPFP Canastell for their great collaboration in the sample collection.

REFERENCES

BAIK H-S, JEON J-M, LEE H-J (2007) Facial soft-tissue analysis of Korean adults with normal occlusion using a 3-dimensional laser scanner. *Am J Orthod Dentofacial Orthop*, 131(6): 759-766.

BANNISTER JJ, JUSZCZAK H, APONTE JD, KATZ DC, KNOTT PD, WEINBERG SM, HALLGRÍMSSON B, FORKERT ND, SETH R (2022) Sex differences in adult facial three-dimensional morphology: application to gender-affirming facial surgery. *Fac Plast Surg Aesthet Med*, 24(S2): S24-S30.

BERGMAN RT (1999) Cephalometric soft tissue facial analysis. *Am J Orthod Dentofacial Orthop*, 116(4): 373-389.

BERMEJO E, TANIGUCHI K, OGAWA Y, MARTOS R, VALSECCHI A, MESEJO P, IBÁÑEZ O, IMAIZUMI K (2021) Automatic landmark annotation in 3D surface scans of skulls: methodological proposal and reliability study. *Comput Methods Programs Biomed*, 210: 106380.

BORMAN H, ÖZGÜR F, GÜRSU G (1999) Evaluation of soft-tissue morphology of the face in 1,050 young adults. *Ann Plast Surg*, 42(3): 280-288.

CAPLE J, STEPHAN CN (2016) A standardized nomenclature for craniofacial and facial anthropometry. *Int J Legal Med*, 130(3): 863-879.

CLAES P, LIBERTON DK, DANIELS K, ROSANA KM, QUILLEN EE, PEARSON LN, MCEVOY B, BAUCHET M, ZAIDI AA, YAO W, TANG H, BARSH GS, ABSHER DM, PUTS DA, ROCHA J, BELEZA S, PEREIRA RW, BAYNAM G, SUETENS P, SHRIVER MD (2014) Modeling 3D facial shape from DNA. *PLoS Genet*, 10(3): e1004224.

COETZEE V, CHEN J, PERRETT DI, STEPHEN ID (2010) Deciphering faces: quantifiable visual cues to weight. *Perception*, 39(1): 51-61.

DONG Y, ZHAO Y, BAI S, WU G, ZHOU L, WANG B (2011) Three-dimensional anthropometric analysis of Chinese faces and its application in evaluating facial deformity. *J Oral Maxillofac Surg*, 69(4): 1195-1206.

ECHEVERRY-QUICENO LM, CANDELO E, GÓMEZ E, SOLÍS P, RAMÍREZ D, ORTIZ D, GONZÁLEZ A, SEVILLANO X, CUÉLLAR JC, PACHAJOA H, MARTÍNEZ-ABADÍAS N (2023) Population-specific facial traits and diagnosis accuracy of genetic and rare diseases in an admixed Colombian population. *Sci Rep*, 13: 6869.

FARKAS LG (1994) *Anthropometry of the head and face*. Raven Press, New York.

FARKAS LG (1996) Accuracy of anthropometric measurements: past, present, and future. *Cleft Palate Craniofac J*, 33(1): 10-18.

FARKAS LG, CHEUNG G (1981) Facial asymmetry in healthy North American Caucasians: an anthropometrical study. *Angle Orthod*, 51(1): 70-77.

FARKAS LG, FORREST CR, LITSAS L (2000) Revision of neoclassical facial canons in young adult Afro-Americans. *Aesthet Plast Surg*, 24(3): 179-184.

FARKAS LG, HRECZKO TA, KOLAR JC, MUNRO IR (1985) Vertical and horizontal proportions of the face in young adult North American Caucasians: revision of neoclassical canons. *Plast Reconstr Surg*, 75(3): 328-337.

FARKAS LG, KATIC MJ, FORREST CR, ALT KW, BAGIC I, BALTADJIEV G, CUNHA E, CVICELOVÁ M, DAVIES S, ERASMUS I, GILLETT-NETTING R, HAJNIS K, KEMKES-GROTTENTHALER A, KHOMYAKOVA I, KUMI A, KGAMPHE JS, KAYO-DAIGO N, LE T, MALINOWSKI A, NEGASHEVA M, MANOLIS S, OGETÜRK M, PARVIZRAD R, RÖSING F, SAHU P, SFORZA C, SIVKOV S, SULTANOVA N, TOMAZO-RAVNIK T, TÓTH G, UZUN A, YAHIA E (2005) International anthropometric study of facial morphology in various ethnic groups/races. *J Craniofac Surg*, 16(4): 615-646.

GENIOLE SN, DENSON TF, DIXSON BJ, CARRÉ JM, MCCORMICK CM (2015) Evidence from meta-analyses of the facial width-to-height ratio as an evolved cue of threat. *PLoS One*, 10(7): e0132726.

GUPTA A, KHARBANDA OP, SARDANA V, BALACHANDRAN R, SARDANA HK (2015) A knowledge-based algorithm for automatic detection of cephalometric landmarks on CBCT images. *Int J Comput Assist Radiol Surg*, 10(11): 1737-1752.

GUROVICH Y, HANANI Y, BAR O, FLEISCHER N, GELBMAN D, BASEL-SALMON L, KRAWITZ P, KAMPHAUSEN SB, ZENKER M, BIRD LM, GRIPP KW (2018) DeepGestalt—Identifying rare genetic syndromes using deep learning. *arXiv*. https://doi.org/10.48550/arXiv.1801.07637

HALLGRÍMSSON B, APONTE JD, KATZ DC, BANNISTER JJ, RICCARDI SL, MAHASUWAN N, MCINNES BL, FERRARA TM, LIPMAN DM, NEVES AB, SPITZMACHER JAJ, LARSON JR, BELLUS GA, PHAM AM, ABOUJAOUDE E, BENKE TA, CHATFIELD KC, DAVIS SM, ELIAS ER, … KLEIN OD (2020) Automated syndrome diagnosis by three-dimensional facial imaging. *Genet Med*, 22(10): 1682-1693.

HEIKE CL, UPSON K, STUHAUG E, WEINBERG SM (2010) 3D digital stereophotogrammetry: a practical guide to facial image acquisition. *Head Face Med*, 6(1): 18.

HEREDIA-LIDÓN Á, ECHEVERRY-QUICENO LM, GONZÁLEZ A, HOSTALET N, POMAROL-CLOTET E, FORTEA J, FATJÓ-VILAS M, MARTÍNEZ-ABADÍAS N, SEVILLANO X (2024) BioFace3D: a fully automatic pipeline for facial biomarkers extraction of 3D face reconstructions segmented from MRI. *arXiv*, 2410.00711.

IMAIZUMI K, TANIGUCHI K, OGAWA Y, MATSUZAKI K, NAGATA T, MOCHIMARU M, KOUCHI M (2015) Three-dimensional analyses of aging-induced alterations in facial shape: a longitudinal study of 171 Japanese males. *Int J Legal Med*, 129(2): 385-393.

JAGADISH CHANDRA H, RAVI MS, SHARMA SM, RAJENDRA PRASAD B (2012) Standards of facial esthetics: an anthropometric study. *J Maxillofac Oral Surg*, 11(4): 384-389.

JAHANSHAHI M, GOLALIPOUR MJ, HEIDARI K (2008) The effect of ethnicity on facial anthropometry in Northern Iran. *Singap Med J*, 49(11): 940-943.

KAHN JL, WOLFRAM-GABEL R, BOURJAT P (2000) Anatomy and imaging of the deep fat of the face. *Clin Anat*, 13(5): 373-382.

KAUR M, GARG RK, SINGLA S (2015) Analysis of facial soft tissue changes with aging and their effects on facial morphology: a forensic perspective. *Egypt J Forensic Sci*, 5(2): 46-56.

KIM SG (2017) Book review for "Orthognathic surgery: principles, planning and practice". *Maxillofac Plast Reconstr Surg*, 39(1): 20.

LEE HY, CHA S, BAN HJ, KIM IY, PARK BR, KIM IJ, HONG KW (2019) The age distribution of facial metrics in two large Korean populations. *Sci Rep*, 9(1): 14564.

LIU J, ROKOHL AC, LIU H, FAN W, LI S, HOU X, JU S, GUO Y, HEINDL LM (2023) Age-related changes of the periocular morphology: a two- and three-dimensional anthropometry study in Caucasians. *Graefes Arch Clin Exp Ophthalmol*, 261(1): 213-222.

MAI HN, KIM J, CHOI YH, LEE DH (2020) Accuracy of portable face-scanning devices for obtaining three-dimensional face models: a systematic review and meta-analysis. *Int J Environ Res Public Health*, 18(1): 94.

MANE DR, KALE AD, BHAI MB, HALLIKERIMATH S (2010) Anthropometric and anthroposcopic analysis of different shapes of faces in group of Indian population: a pilot study. *J Forensic Legal Med*, 17(8): 421-425.

MARTIN R (1957) Lehrbuch der Anthropologie. Dritte Aufl.

MARTOS R, GUERRA R, NAVARRO F, PERUCH M, NEUWIRTH K, VALSECCHI A, JANKAUSKAS R, IBÁÑEZ O (2024) Computer-aided craniofacial superimposition validation study: The identification of the leaders and participants of the Polish-Lithuanian January Uprising (1863-1864). *Int J Legal Med*, 138(1): 107-121.

MATTHEWS HS, MAHDI S, PENINGTON AJ, MARAZITA ML, SHAFFER

JR, WALSH S, SHRIVER MD, CLAES P, WEINBERG SM (2023) Using data-driven phenotyping to investigate the impact of sex on 3D human facial surface morphology. *J Anat*, 243(2): 274-283.

MATTHEWS HS, PENINGTON AJ, HARDIMAN R, FAN Y, CLEMENT JG, KILPATRICK NM, CLAES PD (2018) Modelling 3D craniofacial growth trajectories for population comparison and classification illustrated using sex-differences. *Sci Rep*, 8(1): 4771.

MATTHEWS HS, PALMER RL, BAYNAM GS, QUARRELL OW, KLEIN OD, SPRITZ RA, HENNEKAM RC, WALSH S, SHRIVER M, WEINBERG SM, HALLGRIMSSON B, HAMMOND P, PENINGTON AJ, PEETERS H, CLAES PD (2021) Large-scale open-source three-dimensional growth curves for clinical facial assessment and objective description of facial dysmorphism. *Sci Rep*, 11(1): 12175.

MAYEW WJ (2013) Reassessing the association between facial structure and baseball performance: a comment on Tsujimura and Banissy (2013). *Biol Lett*, 9(5): 20130538.

MENÉNDEZ LÓPEZ-MATEOS ML, CARREÑO-CARREÑO J, PALMA JC, ALARCÓN JA, MENÉNDEZ LÓPEZ-MATEOS C, MENÉNDEZ-NÚÑEZ M (2019) Three-dimensional photographic analysis of the face in European adults from southern Spain with normal occlusion: reference anthropometric measurements. *BMC Oral Health*, 19(1): 196.

MONTÚFAR J, ROMERO M, SCOUGALL-VILCHIS RJ (2018) Hybrid approach for automatic cephalometric landmark annotation on cone-beam computed tomography volumes. *Am J Orthod Dentofacial Orthop*, 154(1): 140-150.

NEELAPU BC, KHARBANDA OP, SARDANA V, GUPTA A, VASAMSETTI S, BALACHANDRAN R, SARDANA HK (2018) Automatic localization of three-dimensional cephalometric landmarks on CBCT images by extracting symmetry features of the skull. *Dentomaxillofac Radiol*, 47(2): 20170054.

OGAWA Y, WADA B, TANIGUCHI K, MIYASAKA S, IMAIZUMI K (2015) Photo anthropometric variations in Japanese facial features: establishment of large-sample standard reference data for personal identification using a three-dimensional capture system. *Forensic Sci Int*, 257: 511.e1-511.e9.

OTHMAN SA, MAJAWIT LP, HASSAN WNW, WEY MC, RAZI RM (2016) Anthropometric study of three-dimensional facial morphology in Malay adults. *PLoS One*, 11(10): e0164180.

OZDEMIR ST, SIGIRLI D, ERCAN I, CANKUR NS (2009) Photographic facial soft tissue analysis of healthy Turkish young adults: anthropometric measurements. *Aesthet Plast Surg*, 33(2): 175-184.

PHAM DD, DO JH, KU B, LEE HJ, KIM H, KIM JY (2011) Body mass index and facial cues in Sasang typology for young and elderly persons. *Evid Based Complement Alternat Med*, 2011: 749209.

RONGO R, SASWAT ANTOUN J, LIM YX, DIAS G, VALLETTA R, FARELLA M (2014) Three-dimensional evaluation of the relationship between jaw divergence and facial soft tissue dimensions. *Angle Orthod*, 84(5): 788-794.

SFORZA C, GRANDI G, CATTI F, TOMMASI DG, UGOLINI A, FERRARIO VF (2009) Age- and sex-related changes in the soft tissues of the orbital region. *Forensic Sci Int*, 185(1): 115.e1-115.e8.

SKOMINA Z, VERDENIK M, HREN NI (2020) Effect of aging and body characteristics on facial sexual dimorphism in the Caucasian population. *PLoS One*, 15(5): e0231983.

TOSTEVIN PM, ELLIS H (1995) The buccal pad of fat: a review. *Clin Anat*, 8(6): 403-406.

VELEMÍNSKÁ J, JAKLOVÁ LK, KOČANDRLOVÁ K, HOFFMANNOVÁ E, KOUDELOVÁ J, SUCHÁ B, DUPEJ J (2022) Three-dimensional analysis of modeled facial aging and sexual dimorphism from juvenile to elderly age. *Sci Rep*, 12(1): 21821.

VIRDI SS, WERTHEIM D, NAINI FB (2019) Normative anthropometry and proportions of the Kenyan-African face and comparative anthropometry in relation to African Americans and North American Whites. *Maxillofac Plast Reconstr Surg*, 41(1): 9.

WEINBERG SM, RAFFENSPERGER ZD, KESTERKE MJ, HEIKE CL, CUNNINGHAM ML, HECHT JT, KAU CH, MURRAY JC, WEHBY GL, MORENO LM, MARAZITA ML (2016) The 3D facial norms database: Part 1. A web-based craniofacial anthropometric and image repository for the clinical and research community. *Cleft Palate Craniofac J*, 53(6): 185-197.

WHITE JD, ORTEGA-CASTRILLÓN A, MATTHEWS H, ZAIDI AA, EKRAMI O, SNYDERS J, FAN Y, PENINGTON T, VAN DONGEN S, SHRIVER MD, CLAES P (2019) MeshMonk: Open-source large-scale intensive 3D phenotyping. *Sci Rep*, 9(1): 6085.